# Image reconstruction from sensitivity encoded MRI data using extrapolated iterations of parallel projections onto convex sets

Alexei A. Samsonov[*a], Eugene G. Kholmovski[b], Chris R. Johnson[a]

[a]Scientific Computing and Imaging Institute, University of Utah, 50 S Central Campus Drive, Room 3490, Salt Lake City, UT, 84112, USA;

[b]Utah Center for Advanced Imaging Research, Department of Radiology, University of Utah, 729 Arapeen Drive, Salt Lake City, UT, 84108, USA

## ABSTRACT

Parallel imaging techniques for MRI use differences in spatial sensitivity of multiple receiver coils to achieve additional encoding effect and significantly reduce data acquisition time. Recently, a projection onto convex sets (POCS) based method for reconstruction from sensitivity-encoded data (POCSENSE) has been proposed. The main advantage of the POCSENCE in comparison with other iterative reconstruction techniques is that it offers a straightforward and computationally efficient way to incorporate non-linear constraints into the reconstruction that can lead to improved image quality and/or reliable reconstruction for underdetermined problems. However, POCSENSE algorithm demonstrates slow convergence in cases of badly conditioned problems. In this work, we propose a novel method for image reconstruction from sensitivity encoded MRI data that overcomes the limitation of the original POCSENSE technique. In the proposed method, the convex combination of projections onto convex sets is used to obtain an updated estimate of the solution via relaxation. The new method converges very efficiently due to the use of an iteration-dependent relaxation parameter that may extend far beyond the theoretical limits of POCS. The developed method was validated with phantom and volunteer MRI data and was demonstrated to have a much higher convergence rate than that of the original POCSENSE technique.

**Keywords:** MRI, sensitivity encoding, image reconstruction, POCS, SENSE, POCSENSE, extrapolated parallel projections, convergence rate

## 1. INTRODUCTION

The long scan times often limit diagnostic efficiency of MRI in many dynamic and physiological studies such as functional, diffusion and perfusion imaging. There are fundamental limitations on the speed of MRI data acquisition due to the technological and physiological limits on the magnetic field gradient switching rate. Over the past few years, a number of parallel imaging techniques exploiting the idea of sensitivity encoding[1-7] have been developed in an attempt to speed up the MRI acquisition. The methods utilize the differences in spatial sensitivity of multiple receiver coils to achieve additional encoding effect that may be used to reduce the number of time-consuming magnetic field gradient encoding steps and, hence, to decrease the data acquisition time. This reduction is achieved by undersampling $k$-space (spatial frequency domain) with a reduction factor $R$. As a result, the significant data acquisition speedup may be achieved without changing image resolution and contrast and utilizing the standard gradient hardware.

Reconstruction from sensitivity-encoded data is usually accomplished with specially developed techniques such as SENSE (SENSitivity Encoding)[1] and SMASH (SiMultaneous Acquisition of Spatial Harmonics)[2]. In SENSE, image reconstruction is accomplished by direct inversion of the encoding matrix. SMASH approximates the inversion by fitting the receiver coil sensitivities to the spatial harmonics. Each method is characterized by a tradeoff among the accuracy of the reconstruction, stability of the solution with respect to noise and systematic errors, and numerical complexity. The quality of the reconstructed images is dependent on a number of factors such as data acquisition

---

* samsonov@sci.utah.edu; phone 1 801 585-0052; fax 1 801 585-6513; http://www.sci.utah.edu; Scientific Computing and Imaging Institute, University of Utah, 50 S Central Campus Drive, Room 3490, Salt Lake City, Utah 84112

reduction factor, the configuration of receiver coil system and accuracy of determination of coil sensitivity profiles. As a rule, linear reconstruction at high and/or maximal reduction factors produces images of poor quality. The standard approach to improve the problem conditioning is to use a priori knowledge about the solution in the form of the constraints. However, inclusion of the majority of non-linear constraints into linear estimation may be both theoretically and numerically problematic. In order to overcome this limitation, a POCS-based method for iterative reconstruction from sensitivity-encoded data (POCSENSE) was previously proposed[8]. The advantage of POCS formulation over linear techniques is that it offers a straightforward and usually computationally non-expensive way to incorporate many non-linear constraints into the reconstruction. In POCSENSE, the available k-space data and constraints are presented as convex sets. Then, the convex combination of simultaneous projections onto the sets is used to obtain an updated estimate of the solution. The flexibility and practical utility of POCSENSE was demonstrated in phase-constrained refinement of images reconstructed from fast spin echo (FSE) data[9]. Under the phase smoothness assumption, the refined phase image was used as the constraining convex set. The use of this constraint leads to a major improvement of image reconstruction for high and/or maximal reduction factors.

The original POCSENSE technique suffers from slow convergence that is typical for the majority of POCS-based reconstruction methods. The convergence of POCSENSE becomes extremely slow for badly conditioned problems such as reconstruction from highly undersampled data. The slow convergence seriously limits application of POCSENSE in many practical situations. In this work, we propose a novel method for image reconstruction from sensitivity encoded MRI data that overcomes the limitation of the original POCSENSE technique. The new method is based on extrapolated iterations of parallel projections onto convex sets[10]. The method converges very efficiently due to the use of an iteration-dependent relaxation parameter that may extend well beyond the traditional range of (0, 2]. The proposed method was tested with phantom and volunteer data. The results indicate that the convergence rate of the new method is significantly (up to an order of magnitude) higher than that of the original POCSENSE algorithm.

## 2. THEORY

### 2.1 Sensitivity encoding in MRI

In multicoil MRI acquisition, several receiver coils ($i=1, \ldots, N_C$) with spatially non-uniform coil sensitivity profiles $s_i(r)$ are positioned around the object to simultaneously acquire data in k-space. The signal $m_i(k)$ obtained from receiver coil $i$ could be considered as a projection of an image function $f(r)$ against hybrid encoding functions that are products of sinusoidal modulation due to the magnetic field encoding gradients and receiver coil sensitivity profile[3]:

$$m_i(k) \propto \int f(r)s_i(r)e^{j2\pi r k(t)}dr \,, \tag{1}$$

where $r$ and $k$ are the image space and k-space coordinates respectively. Equation [1] could be presented in discretized matrix form as

$$\mathbf{E}^{(i)}\mathbf{f} = \mathbf{m}^{(i)} \,, \tag{2}$$

where $\mathbf{E}^{(i)}$ is the *encoding* matrix and $\mathbf{m}^{(i)}$ is the data vector for coil $i$. The matrices for all coils could be stacked to form full encoding matrix $\mathbf{E}$ and the data vector $\mathbf{m}$ as follows:

$$\mathbf{E} = \begin{bmatrix} \mathbf{E}^{(1)} \\ \vdots \\ \mathbf{E}^{(N_C)} \end{bmatrix}, \ \mathbf{m} = \begin{bmatrix} \mathbf{m}^{(1)} \\ \vdots \\ \mathbf{m}^{(N_C)} \end{bmatrix} \tag{3}$$

and then used to form the final matrix equation

$$\mathbf{E}\mathbf{f} = \mathbf{m} \,. \tag{4}$$

Each row of the system corresponds to a single k-space point for a given receiver coil. For a multicoil acquisition, the system is overdetermined and, hence, the number of k-space points to acquire could be traded for accuracy of the least
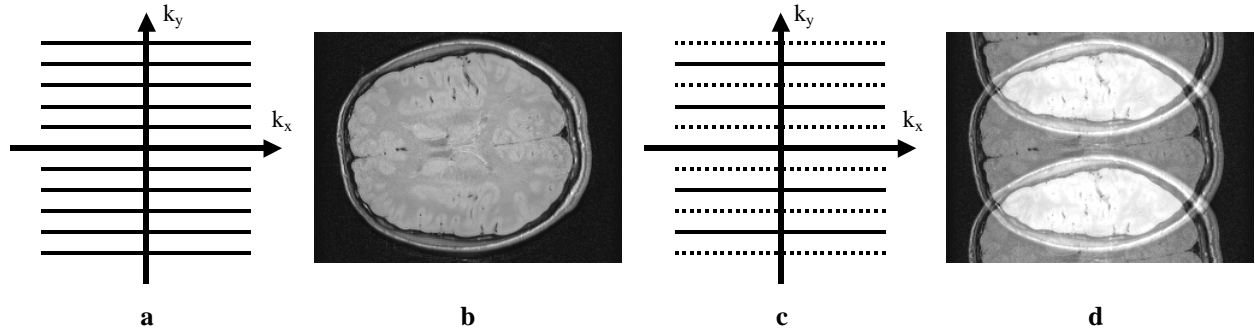
Figure 1: (a) Fully sampled *k*-space and (b) corresponding image, (c) regularly undersampled Cartesian *k*-space with every second line omitted (R=2) and (d) corresponding image corrupted by aliasing artifact.

mean squares (LMS) estimation of the image vector **f**. The LMS estimation amounts to solving the set of the normal equations:

$$\mathbf{E^H E f = E^H m} \,,$$ (5)

where **H** is Hermitian conjugate operation.

The most efficient way to reduce the number of the magnetic field gradient encoding steps is *k*-space undersampling that is charactirized by the reduction factor *R*. Acquisition schemes for full Cartesian sampling and uniform undersampling with reduction factor *R=2* are shown on Fig. 1. Theoretically, the LMS solution of the reconstruction problem is attainable up to the reduction factors $R=N_C$. The thourough theoretical treatment of the reconstruction problem may be found in several studies[1,3]. It should be noted that the reconstruction requires a knowledge of the coil sensitivity profiles.

The image reconstructed by direct inversion of the encoding matrix has increased and spatially non-uniform noise level. At high reduction factors, the matrix condition number is large and may lead to substantial amplification of the noise component of the signal causing severe degradation of image quality. In those cases, a priori knowledge about final image properties such as limited region of support, highest attainable image intensity value or smoothness of image phase may be used to improve the reconstruction quality. Unfortunately, the straightforward inclusion of such nonlinear constraints into the linear reconstruction is generally problematic.

## 2.2 Image reconstruction using projections onto convex sets (POCS)

POCS theory offers a powerful mathematical apparatus for solving many reconstruction problems that involve incomplete and/or inconsistent data. The main advantage of POCS is that it presents a natural way to incorporate a priori knowledge into the reconstruction process. The conceptual basis of POCS is that both linear and nonlinear constraints onto the final image and available data measurements can be often represented as convex sets in a Hilbert space, *H*, where each element of *H* is an image. A set of points $\Omega \in H$ is considered to be convex if and only if for any $f_1, f_2 \in \Omega$ the element $f = \alpha f_1 + (1-\alpha) f_2$ is also found in $\Omega$ ($f \in \Omega$) for all $\alpha \in [0,1]$. In case of the image reconstruction problem, every known constraint on the image *f* restricts it to lie in the associated closed convex subset of *H*. If *n* such constraints are available, *n* closed convex sets $\Omega_i$ (*i*=1, …, *n*) may be generated. Any point of intersection $\Omega_0 = \cap \Omega_i$ may be considered to be the solution of the reconstruction problem as it satisfies all the represented constraints and the data.
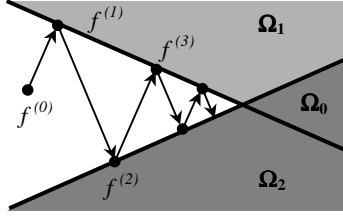
Figure 2: Illustration of convergence of POCS iterations (Eq. [8]) for two convex sets $\Omega_1$ and $\Omega_2$ with a non-empty intersection $\Omega_0$. Starting with some initial guess $f^{(0)}$, the series of the projections brings the estimate closer to a solution point in $\Omega_0$.
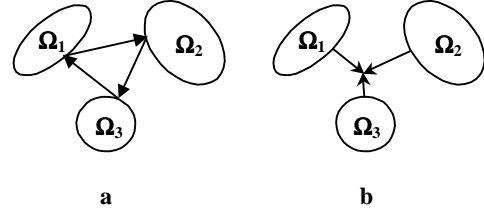
Figure 3: Convergence of sequential (**a**) and parallel (**b**) POCS algorithms in case of inconsistent convex sets. As $\Omega_0$ is empty, the sequential POCS exhibits periodic behavior with the solution satisfying the constraints unevenly. For parallel POCS, the solution is a fixed point.

The problem of finding a point in $\Omega_0$ could be recursively solved, if each convex set $\Omega_i$ ($i$=1, ..., $n$), has the assosiated projection operator $P_i$ that projects the current image estimate on the closest point in $\Omega_i$. In more general form, the relaxed projection operator can be defined by

$$T_i = I + \lambda_i (P_i - I),$$
(6)

where $I$ is the identity operator and $\lambda_i$ is a relaxation parameter defined in the range of (0,2]. Then, the solution could be found by the sequence of alternating projections onto the convex sets as

$$f^{(m+1)} = T_1 .. T_n f^{(m)}.$$
(7)

If $\Omega_0$ is not empty and every $\lambda_i \in (0,2]$, the fundamental theorem of POCS[11] guaranties weak convergence to a point in $\Omega_0$ (Fig. 2). As the projections in Eq. [7] follow each other, this method is further referred to as *sequential POCS*.

The sequential POCS has a number of shortcomings. First, it is characterized by slow convergence. Second, the application of the sequential POCS to the problem with multiple and inconsistent constraints is limited. The convex sets defined by the available data and the constraints may be inconsistent due to the measurement noise or other errors. The intersection of such inconsistent convex sets is an empty set. The convergence of sequential POCS to a fixed point is no longer guaranteed. When $\Omega_0$ is an empty set, the sequential algorithm converges to a closed path called a greedy limit cycle and stays on the path indefinitely (Fig. 3a). Thus, the obtained solution does not satisfy all the expected solution properties.

In cases of inconsistent convex sets, parallel POCS algorithms such as the method of extrapolated parallel projections (EPPM)[10] have more desirable characteristics. At each iteration of EPPM, projections $P_i\left(f^{(n)}\right)$ of the current solution estimate onto all available convex sets are calculated in parallel and then convexly combined:

$$a^{(n)} = \sum_i w_i P_i\left(f^{(n)}\right),$$
(8)

where $\sum_i w_i = 1$. The extrapolation parameter $L^{(n)}$ is found as

$$L^{(n)} = \frac{\sum_i w_i \left\| P_i\left(f^{(n)}\right) - f^{(n)} \right\|^2}{\left\| \sum_i w_i P_i\left(f^{(n)}\right) - f^{(n)} \right\|^2}$$
(9)

and used to update the image estimate:

$$f^{(n+1)} = f^{(n)} + \lambda^{(n)}(a^{(n)} - f^{(n)}),$$

(10)

where $\lambda^{(n)} \in (0, 2L^{(n)}]$.

Parallel POCS algorithms are more robust than the conventional sequential POCS methods. In cases of inconsistent convex sets, the parallel POCS algorithm converges weakly to a point in a Hilbert space such that the weighted least squares distance between the point and all convex sets is minimized[10,12] (Fig. 3b). This outcome is more preferable than that of the greedy circling of the sequential POCS, because the found solution is close to each of the convex sets and, therefore, all constraints on the solution give contributions to the final result. Another important advantage of EPPM is its efficient convergence. This is evident from the fact that in EPPM the relaxation parameter is adaptively adjusted after each iteration and its value may extend well beyond the range of (0, 2]. The method presented in the paper belongs to the family of the EPPM algorithms.

## 3. METHODOLOGY

### 3.1 Definition of the convex sets and corresponding projection operators

Let $r$ and $k$ be the image space and $k$-space coordinates respectively, $s_i(r)$ and $S_i(k)$ - $i$-th coil sensitivity profile and its Fourier transform, $f(r)$ and $F(k)$ - the image function and its Fourier transform, $\tilde{K}$ - the $k$-space sampling pattern and $m_i(k)$ - data acquired by the $i$-th coil at $k \in \tilde{K}$. The convex sets and the corresponding projection operators are defined as follows:

1. $\Omega_{data}^i, i = 1, ..., N_C$ (set of images with $k$-space values at $k \in \tilde{K}$ equal to $m_i(k)$; main or data convex set)

$$P_{data}^i g(r) \Leftrightarrow \begin{cases} m_i(k), & k \in \tilde{K} \\ G(k), & k \notin \tilde{K} \end{cases}$$

The projection operator is essentially the data substitution operator that ensures that after the projection onto the set the $k$-space of the image $g(r)$ will have the predefined values $m_i(k)$ at the sampled positions $k \in \tilde{K}$.

2. $\Omega_M$ (set of images with object support area $M$; optional convex set)

$$P_M f(r) = \begin{cases} f(r), & r \in M \\ 0, & otherwise \end{cases}$$

The projection operator zeroes values outside object support area $M$.

3. $\Omega_V$ (set of images with maximum intensity value $V$; optional convex set)

$$P_V f(r) = \begin{cases} f(r), & f(r) \leq V \\ V, & otherwise \end{cases}$$

The projection operator restricts the image intensity value to be lower or equal to the predefined value $V$.

4. $\Omega_\phi$ (set of images with image phase $\phi$; optional convex set)

$$P_\phi f(r) = |f(r)| \cdot e^{i\phi(r)}$$

The projection operator sets the image phase to the predefined function $\phi(r)$.

Other optional convex sets and projection operators could be constructed if other a priori information about the solution of the image reconstruction problem is available.

## 3.2 Algorithm

Let $\|\cdot\|$ denote $L2$ norm, "*" - complex conjugation and $P_{OPT}$ - a series of consequent projections on all the available optional convex sets as defined in Sec. 3.1.

Starting with some initial guess $f^{(0)}$, iterate until the convergence criteria is met:

Step 1. Projection onto data sets:

$$g_i = P_{data}^i(s_i f^{(n)}), \, i = 1,..., N_C.$$

Step 2. Linear combination of individual coil images:

$$g_0 = \frac{\sum_{i=1}^{N_C} g_i s_i^*}{\sum_{i=1}^{N_C} |s_i|^2}.$$

Step 3. Projection onto the optional convex sets:

$$g^{(n+1)} = P_{OPT}(g_0).$$

Step 4. Calculations of the extrapolation parameter and the relaxation coefficient:

$$L^{(n)} = \frac{\sum_{i=1}^{N_C} \left\| g_i s_i^* - f^{(n)} |s_i|^2 \right\|^2}{\left\| (g_0 - f^{(n)}) \cdot \sum_{i=1}^{N_C} |s_i|^2 \right\|^2},$$

$$\varepsilon \leq \lambda^{(n)} \leq (2-\varepsilon)L^{(n)}, \quad (0 \leq \varepsilon \leq 1).$$

Step 5. Calculation of the image estimate:

$$f^{(n+1)} = f^{(n)} + \lambda^{(n)} \left( g^{(n+1)} - f^{(n)} \right).$$

At each iteration $n$, the current image estimate is projected in parallel onto subgroups of the data convex sets (Step 1) and the results are then combined using known coil sensitivity profiles (Step 2). After additional projections on the available optional convex sets are accomplished (Step 3), the extrapolation coefficient $L^{(n)}$ and the relaxation parameter $\lambda^{(n)}$ are found (Step 4) and used to update the image estimate (Step 5). The iterations are stopped when convergence criterion is met.

## 3.3 Implementation details

The main computational load of the algorithm is on Step 1. For each coil, the product of the current image estimate with the corresponding coil sensitivity profile is transferred into the spatial-frequency domain using fast Fourier transform (FFT), then the acquired $k$-space data are substituted and the result is transferred back into the image space using inverse FFT (IFFT). FFT and IFFT are fast algorithms with complexity of order $O(N^2 logN)$ for the 2D case that could be efficiently implemented in hardware. Furthermore, the processing of Step 1 could be organized in parallel processing each data convex set independently.

Since accurate knowledge of the individual coil sensitivities is essential for artifact-free reconstruction of sensitivity encoded MRI data, a method for reliable determination of coil sensitivity maps is required. The sensitivity maps are

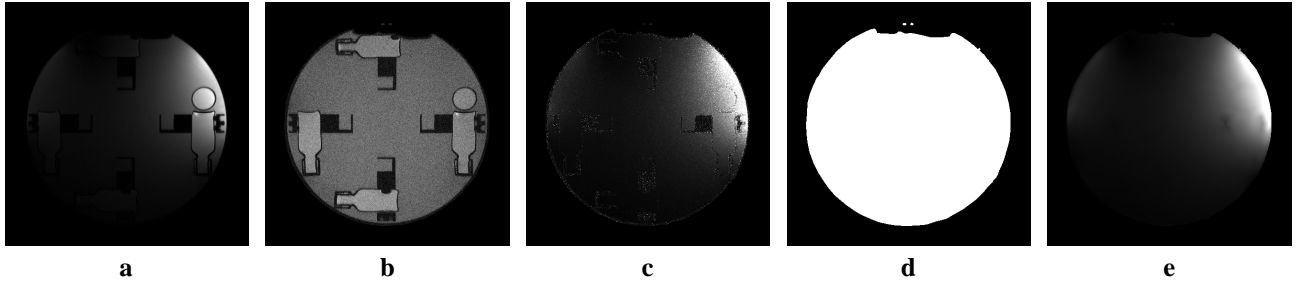|       |       |       |       |       |
|:-----:|:-----:|:-----:|:-----:|:-----:|
| a | b | c | d | e |

Figure 4. Illustration on the sensitivity map determination procedure used in the experiments. The ratio between an individual surface coil image (a) and a body coil image (b) gives the surface coil sensitivity estimate (c). The object support mask (d) is generated using the thresholding of the reference image. To denoise the estimate, a local polynomial fit is applied in the limits of the object mask to get a smoothed sensitivity map (e).

usually extracted from reference scans acquired prior to sensitivity-encoded imaging. As a rule, two reference scans are required: one with the coil having close to uniform sensitivity (e.g. body coil), and the other scan with the surface coil array whose sensitivity maps estimation is needed. The reference scan based method for coil sensitivity estimation is described in detail in[1] and illustrated on Fig. 4. Alternative approach to coil sensitivity estimation is to use self-calibrating acquisition schemes[13].

The optional constraints for the reconstruction from the sensitivity-encoded data are the object spatial support and the maximum attainable image value. The object support area and image maximum value may be obtained analyzing low-resolution reference image used for coil sensitivity estimation.

## 4. DATA

Validation of the developed method for image reconstruction from sensitivity-encoded data was accomplished studying its feasibility and effectiveness on data from phantom and human volunteer studies. Informed consent was obtained from all volunteers in accordance with our institution's human subjects policies. All imaging studies were performed on a 1.5 Tesla GE SIGNA MR scanner (General Electric Medical Systems, Waukeesha, WI) with NV/CVi gradients (40 mT/m amplitude, 150 mT/m/ms slew rate) using a custom-built four-element ($N_c$=4) bilateral temporal lobe phased array coil[14].

Sensitivity encoded data were acquired immediately after the reference scans. In the phantom studies, a uniform undersampling scheme with reduction factor $R$=4 was realized by acquiring only every fourth line in $k$-space. The coil
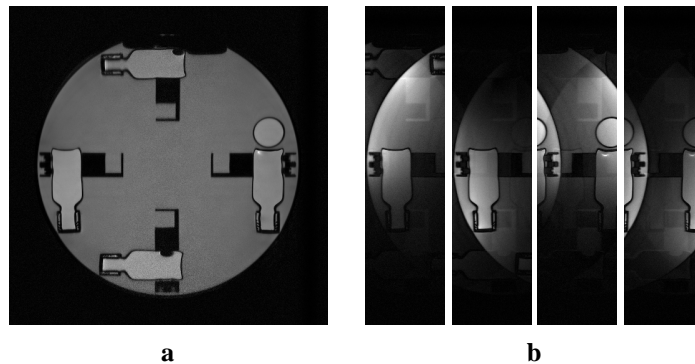


|   |   |
|:-:|:-:|
| a | b |

Figure 5. Phantom (a) used in the experiments and individual coil images (b) obtained with reduction factor $R$=4.

images reconstructed from the data are shown in Fig. 5. The images manifest an aliasing (folding) in the phase-encoding direction. Four data sets (one per each coil array element) and a compact object support (Fig. 4d) were used in the reconstruction of phantom images.

Both fully sampled and undersampled $T_2$-weighted data of a volunteer brain were acquired using a FSE imaging technique. The $k$-space data were uniformly undersampled with reduction factor $R$=4 maximal for the given number of coils. Coil data sets, compact object support and smoothed phase estimate were used in the reconstruction of brain images. Methodic of obtaining the phase estimate is described in the Results section of the paper.

## 5. RESULTS

The reconstruction of phantom data was performed with both POCSENSE and the proposed method. For error measurement, the reference image $f_0$ was obtained using SENSE reconstruction, i.e. reconstruction by direct inversion of the corresponding matrix equation (Eq. [5]). The both iterative methods should be converging to the image $f_0$. At each iteration $n$, the error was measured as

$$err^{(n)} = \frac{\left\| f^{(n)} - f_0 \right\|}{\left\| f_0 \right\|} . \tag{11}$$

The results of reconstruction after 70 iterations are presented on Fig. 6. The image reconstructed by extrapolated parallel projections (Fig. 6a) does not contain noticeable aliasing artifact, while the image reconstructed by POCSENSE (Fig. 6b) using the same number of iterations suffers from significant residual aliasing. The convergence behavior of the methods for the reconstruction is presented in Fig. 7. The results indicate that the convergence rate of the new method is significantly (up to an order of magnitude) higher than that of the original POCSENSE algorithm.

The proposed method was used for phase-constrained refinement of images reconstructed by the standard SENSE method. First, the initial images (Fig. 8b) were reconstructed with SENSE from sensitivity encoded brain data. The images reconstructed by the SENSE method show a significant noise contamination (Fig. 8b). This outcome is typical for SENSE reconstruction from highly undersampled data acquired with a non-optimized coil system. The degradation of image signal-to-noise ratio (SNR) due to the SENSE reconstruction is described by a spatially variable *geometry factor*[1]. Figure 8c demonstrates that the proposed method with an additional phase smoothness constraint may significantly improve the resulting image quality in comparison with the image reconstructed by the standard SENSE algorithm. In this study, the image phase constraint was obtained extracting the phase of the low-resolution part of the SENSE images. Then, it was used as an additional convex set as explained in Sec. 3.1.
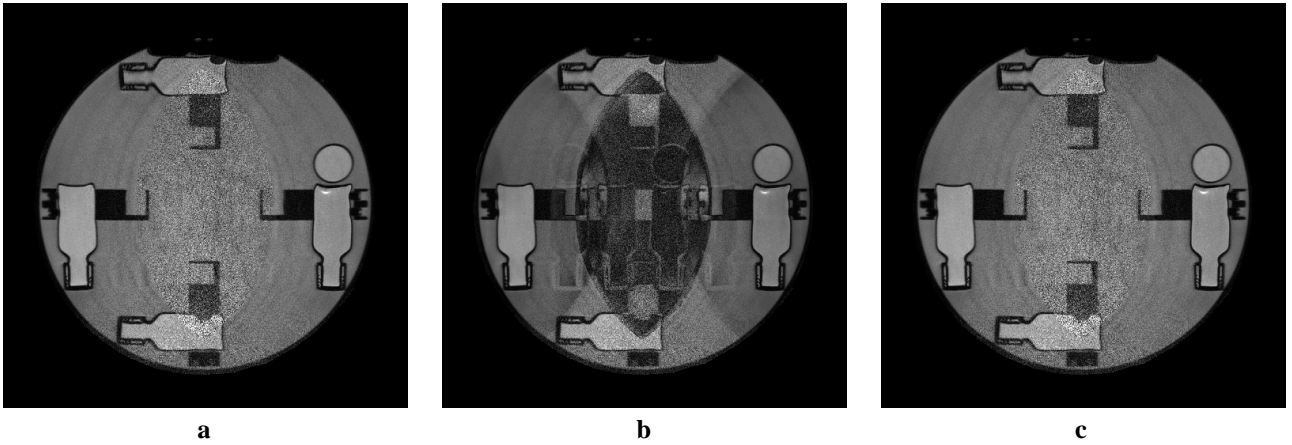


|  a  |  b  |  c  |

Figure 6: Reconstruction from sensitivity encoded phantom data. a) Image reconstructed by extrapolated parallel projections ($\lambda^{(n)}$=1.5$L^{(n)}$, after 70 iterations), b) Image reconstructed by POCSENSE (after 70 iterations), c) Image reconstructed by direct inversion of the matrix equation (Eq. [5]).
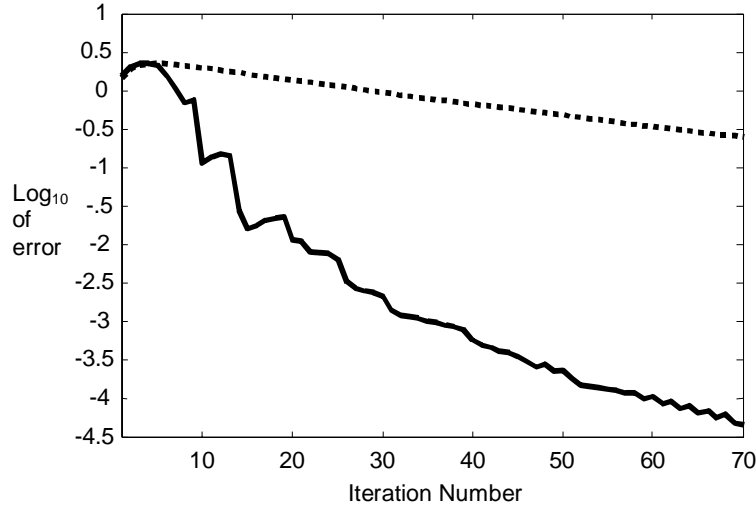
Figure 7: Reconstruction error for the proposed method (solid) and POCSENSE (dotted) for the phantom image reconstruction (Fig. 6).
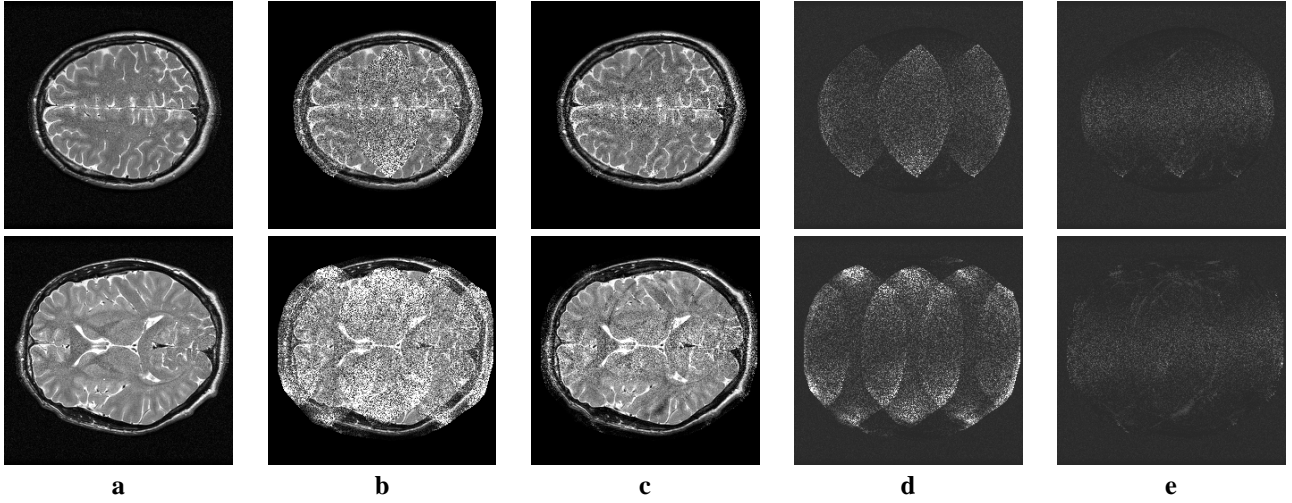


Figure 8. Phase-constrained refinement using extrapolated parallel projections. a) Reference images obtained from fully sampled k-space, b) images reconstructed with SENSE ($R$=4), c) images obtained by the proposed method ($\lambda^{(n)}=1.5L^{(n)}$, 50 iterations) with the image phase constraint, d) the magnitude of difference between images (a) and (b), e) the magnitude of difference between images (a) and (c).

In order to visually evaluate the quality of reconstruction, the absolute differences between the reference (Fig. 8a) and reconstructed images were calculated. The difference images (Fig. 8d,e) indicate that the proposed method with phase-smoothness constraint provides noticeable improvement in the image quality. The refined images (Fig. 8c) contain many important anatomical structures that are missing in SENSE image (Fig. 8b). Minor aliasing artifacts present in the refined images arise because of errors in coil sensitivity profile estimates and violation of the phase smoothness on the tissue-air interface areas.

# 6. CONCLUSIONS

POCS-based methods offer flexibility of using the wide range of constraints that made them attractive for many problems of image reconstruction from insufficient and/or corrupted data. The images reconstructed from sensitivity encoded MRI data with high/maximal reduction factors usually have poor image quality. POCS-based methods have a potential to improve the quality in many such cases when a priori knowledge about the image properties is available.

We developed the novel POCS-based method for image reconstruction from sensitivity-encoded MRI data. The method overcomes the limitations of the sequential POCS-based methods such as slow convergence and non-reliable reconstruction with multiple constraints. The method provides a much higher convergence rate compared to the original POCSENSE method, especially for extreme cases of high and/or maximal reduction factors and non-optimal coil geometry. The flexibility of the proposed technique allows for improved image reconstruction when additional constraints are available. The method could be very efficiently implemented in parallel using FFT algorithm. Along with fast convergence and flexibility, this makes the new method attractive for reconstruction of images from sensitivity encoded MRI data in clinical environments.

## REFERENCES

1. K.P. Pruessmann, M. Weiger, M.B. Scheidegger, and P. Boesiger, "SENSE: Sensitivity Encoding for Fast MRI," *Magn Reson Med*, **42**, pp. 952–962, 1999
2. D.K. Sodickson and W.J. Manning, "Simultaneous acquisition of spatial harmonics (SMASH): ultra-fast imaging with radiofrequency coil arrays," *Magn Reson Med*; **38**, pp. 591–603, 1997
3. D.K. Sodickson and C.A. McKenzie, "A generalized approach to parallel magnetic resonance imaging," *Med Phys*, **28**, pp. 1629-1643, 2001
4. M.A. Griswold, P.M. Jakob, R.M. Heidemann, M. Nittka, V. Jellus, J. Wang, B. Kiefer, and A. Haase, "Generalized autocalibrating partially parallel acquisition (GRAPPA)," *Magn Reson Med*, **47**, pp. 1202-1210, 2002
5. M. Bydder, D.J. Larkman, J.V. Hajnal, "Generalized SMASH imaging," *Magn Reson Med*, **47**, pp. 160-170, 2002
6. M.A. Griswold, P.M. Jakob, R.M. Heidemann, A. Haase. "Parallel imaging with localized sensitivities (PILS)," *Magn Reson Med*, **44**, pp. 243-251, 2000
7. W.E. Kyriakos, L.P. Panych, D.F. Kacher, C.F. Westin, S.M. Bao, R.V. Mulkern, F.A. Jolesz, "Sensitivity profiles from an array of coils for encoding and reconstruction in parallel (SPACE RIP)," *Magn Reson Med*, **44**, pp. 301-308, 2000
8. E.G. Kholmovski, A.A. Samsonov, and D.L. Parker, "POCSENSE: POCS-Based Reconstruction Method for Sensitivity Encoded Data," *Proceedings of ISMRM 2002*, p. 194, Honolulu, 2002
9. A.A. Samsonov, and E.G. Kholmovski, "Method for Quality Improvement of Images Reconstructed From Sensitivity-Encoded Data," *Proceedings of ISMRM 2002*, p. 2408, Honolulu, 2002
10. P.L. Combettes, "Convex set theoretic image recovery by extrapolated iterations of parallel subgradient projections," *IEEE Trans Image Processing*, **6**, pp. 493-506, 1997
11. L.G. Gubin, B.T. Polyak, and E.V. Raik, "The method of projections for finding the common point in convex sets," *USSR Comput Math Phys*, **7**, pp. 1-24, 1967
12. P.L. Combettes, "Inconsistent signal feasibility problems: Least-squares solutions in a product space," *IEEE Trans Signal Processing*, **42**, pp. 2955-2966, 1994
13. C.A. McKenzie, E.N. Yeh, M.A. Ohliger, M.D. Price, and D.K. Sodickson, "Self-calibrating parallel imaging with automatic coil sensitivity extraction," *Magn Reson Med*, **47**, pp. 529-538, 2002
14. J.R. Hadley, B.E. Chapman, J.A. Roberts, D.C. Chapman, K.C. Goodrich, H.R. Buswell, A.L. Alexander, J.S. Tsuruda, and D.L. Parker, "A three-coil comparison for MR angiography," *J Magn Reson Imaging*, **11**, pp. 458-468, 2000